

# A New Mechanistic Model to Predict Gas–Liquid Interface Shape of Gas–Liquid Flow Through Pipes with Low Liquid Loading

Ahmad Banafi and Mohammad Reza Talaie

Dept. Chemical Engineering, Faculty of Engineering, University of Isfahan, Isfahan, Iran

Mohammad Reza Talaie

Dept. Chemical and Environmental Engineering, Faculty of Engineering, University of Nottingham Malaysia Campus, Semenyih, Malaysia

DOI 10.1002/aic.14696

Published online December 2, 2014 in Wiley Online Library (wileyonlinelibrary.com)

*Devising a new mechanistic method to predict gas–liquid interface shape in horizontal pipes is concerned in this article. An experiment was conducted to find the pressure gradients of air–water flow through a 1-in. pipe diameter. Comparing results of model with some experimental data available in the literature demonstrates that the model provides quite better predictions than existed models do. This model also predicts flow regime transition from stratified to annular flow better than Apparent Rough Surface and Modified Apparent Rough Surface models for both 1- and 2-in. pipe diameters. The model also leads to reliable predictions of wetted wall fraction experimental data. Although one parameter of new model was evaluated based on air–water flow pressure loss experimental data for 1 in. pipe, it was considerably successful to predict pressure drop, liquid holdup, stratified-annular transition and wetted wall fraction for other gas–liquid systems and pipe diameters. © 2014 American Institute of Chemical Engineers AICHE J, 61: 1043–1053, 2015*

**Keywords:** two-phase flow, mechanistic model, liquid holdup, pressure drop, gas, liquid interface

## Introduction

In natural gas transmission, even when the gas input is in single-phase state, liquid may be formed in the pipelines due to retrograde condensation as a result of pressure drop.<sup>1</sup> Although the liquid loading is low for this case, the range of liquid holdup could be varied vastly between 0.005 and 0.4 depending on inclination angle of pipeline. The presence of traces of liquid causes considerable increase in pressure drop along the pipeline.<sup>2</sup> At low gas flowrates, the wall layer may cover only part of the pipe periphery but, at higher flowrates, the liquid can cover the whole of the periphery. The latter case is horizontal annular flow and the former case has been referred to as partially annular flow or stratified-wavy flow.<sup>3</sup> Stratified flow is the dominant flow pattern of low liquid loading gas–liquid flow in horizontal pipes.<sup>1</sup>

Accurate predictions of pressure loss and liquid holdup are vital in gas–condensate pipeline design. Many attempts have been made to develop empirical correlations and phenomenological models for predicting pressure drop and liquid holdup in gas–liquid flows through pipes. The implied objective of all these studies has been to develop gas–liquid flow models which are capable of making accurate prediction in field condition while they are tuned based on laboratory data. In other words, these models play the role of

extrapolation functions to extrapolate field-condition data from the laboratory-condition ones. The early studies such as Lockhart and Martinelli,<sup>4</sup> Hughmark,<sup>5</sup> and Beggs and Brill<sup>6</sup> focused on introducing empirical correlations for prediction of pressure drop and liquid holdup in a relatively large range of liquid holdups. Whilst, the second-generation models including Taitel and Dukler,<sup>7</sup> Olimans,<sup>8</sup> Cheremisinoff and Davis,<sup>9</sup> Shoham and Taitel,<sup>10</sup> Hamersma and Hart,<sup>11</sup> Issa,<sup>12</sup> Baker et al.,<sup>13</sup> Hart et al. Apparent Rough Surface (ARS),<sup>2</sup> Chen et al.,<sup>14</sup> Grolman and Fortuin Modified Apparent Rough Surface models (MARS),<sup>15</sup> Vlachos et al.,<sup>16</sup> Asante et al.,<sup>17</sup> Meng et al.,<sup>18</sup> Talaie and Deilamani,<sup>19</sup> and Fan<sup>20</sup> have been developed based on the physical facts of two-phase flow phenomena to some extent. Because of the complexity of the phenomena occurring in gas–liquid flow through a pipe, roughly simplifying assumptions were made to develop these mechanistic models.<sup>3</sup> These gross assumptions have resulted in inaccurate predictions. The main differences among these models include applying different correlations for predicting friction factors and using various ways for determining gas–liquid interface shape. Thus, friction factors (gas–wall, liquid–wall and gas–liquid tensions) and interface shape are the most influencing parameters in accurate prediction of pressure loss and liquid holdup in horizontal gas–liquid pipe flow with low liquid loading.

Taitel and Dukler<sup>7</sup> proposed a generalized one-dimensional two-fluid model which has been served as the basis of many other models introduced in the literature since then. In this model, it was assumed that the gas–liquid

Correspondence concerning this article should be addressed to Mohammad Reza Talaie at Mreza.Talaie@Nottingham.edu.my or mrtalaiekh@yahoo.com

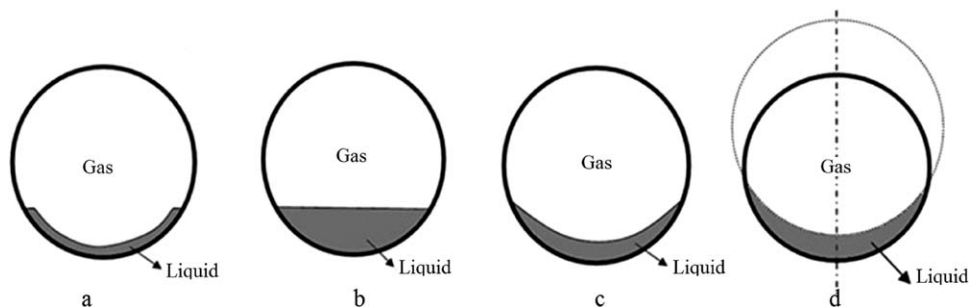


**Figure 1. Liquid layer shape assumed in different models.**

(a) Thin film; Hamersma and Hart,<sup>11</sup> (b) flat surface; Taitel-Dukler,<sup>7</sup> (c) curved surface; Grolman and Fortuin,<sup>15</sup> (d) double circle; Chen et al.<sup>14</sup>

interface was flat. Hamersma and Hart<sup>11</sup> assumed that liquid flowed as a thin film on the pipe inside wall. The influence of this film is modifying wall roughness and effective diameter of the pipe. It was claimed that the model was applicable for the liquid holdups up to 0.04. Chen et al.<sup>14</sup> have predicted gas-liquid interface shape as a part of imaginary large circle which lies between the intersection points with the pipe cross section circumference. The center of the imaginary circle was determined using a correlation, and its radius was equal to the distance between the center and the end points of the wetted perimeter on the pipe wall as shown in Figure 1d. Grolman and Fortuin<sup>15</sup> considered an important fact in development of their model. Their experimental studies showed that in wavy gas-liquid pipe flow, liquid creeps up against the inside pipe wall. Although this effect has been rarely accounted in literature, it significantly affects the interfacial perimeters  $S_i$ ,  $S_L$ , and  $S_G$  as well as the interfacial friction factor  $f_i$ . For prediction of interfacial perimeter,  $S_i$ , Grolman and Fortuin used a linear interpolation between a minimum value of  $S_i$  [ $D \sin(\pi\theta_0)$ ] for flat surface and the one [ $(1-\alpha)^{0.5}\pi D$ ] for cylindrically symmetric, closed annular flow ( $\theta=1$ ) to determine the interface area. Figure 1 demonstrates the different gas-liquid configurations used in aforementioned models. It should be noted that all these models are applicable only in stratified flow regime.

Different models which have been proposed so far for prediction of pressure drop and liquid holdup in gas-liquid flows with low liquid loading do not provide reliable predictions, especially in relatively higher values of liquid holdup.

An inescapable fact observed in the models existed in the literature is the lack of a realistic view of gas-liquid interface shape in gas-liquid flow with low liquid loading. This article was aimed at devising a more accurate way to characterize gas-liquid interface shape. This shape was determined based on the physical rules underlying gas-liquid flow phenomena. In this model, liquid-phase velocity distribution is recognized as the immediate cause for transformation of a flat interface into a curved one.

## Experiment

A setup was designed and assembled to perform experimental measurement of pressure drop on gas-liquid flow with low liquid loading. Figure 2 shows the schematic diagram of this setup. It consists of a horizontal plastic tube with 7 m long and 1 in. internal diameter, a micromanometer, air compressor, damping tank, water supply tank, and cyclone. Water is pumped from water source to the water supply tank to make up the water flowing through the pipe. To maintain a constant water flow rate, this tank is

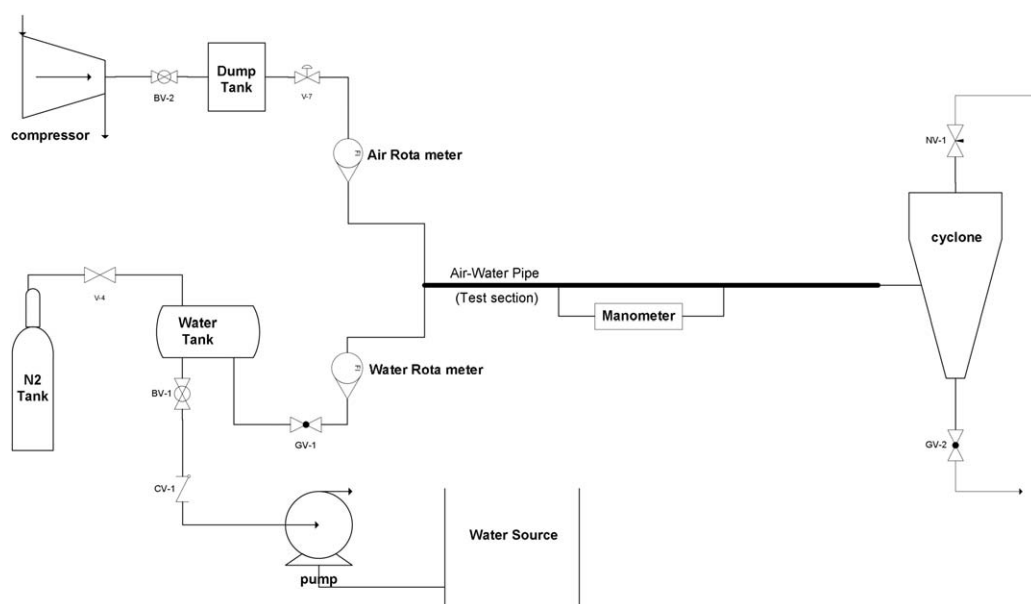


**Figure 2. Schematic diagram of designed setup.**

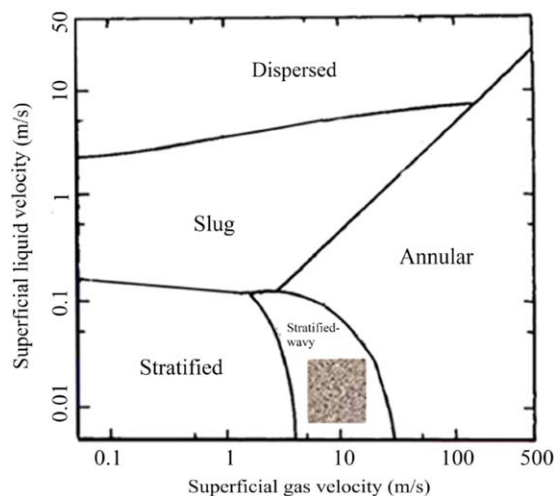


**Figure 3. The conditions of the performed experiments marked on the flow pattern map.**

[Color figure can be viewed in the online issue, which is available at [wileyonlinelibrary.com](http://wileyonlinelibrary.com).]

pressurized using nitrogen gas at a constant pressure of 5 bar. The compressed air with pressure of 8–10 bar coming from a compressor is sent to a tank to damp the pressure fluctuations. The compressed air flowing into the pipe is supplied from this tank through a gas regulator to adjust the pressure and flow rate. Air and water are fed to the test section concurrently at the pressures between 1 and 3 bar. In the end of the test section, air and water enter a cyclone and separate from each other. The air flow rate is measured using a flow meter calibrated for ranging from 2 to 30 m<sup>3</sup>/h with the precision of 3%. The water flow rate is also metered through a water flow meter calibrated for ranging from 16 to 80 L/h with the precision of  $\pm 1$  L/h. The pressure difference was measured between the distance of 2.5 m along the pipe using an inclined manometer with an accuracy of  $\pm 1$  pa. The range of gas and liquid superficial velocities covered in this experiment is presented by the shaded area located on Taitel–Duckler flow regime map<sup>7</sup> as shown in Figure 3. As can be seen from this figure, the flow pattern maintain in stratified-wavy regime through whole experiment.<sup>21</sup>

## Mathematical Model

### Gas liquid configuration

The flat gas–liquid interface shape assumed by Taitel–Dukler<sup>7</sup> is consistent with reality when the gas and liquid are nearly at rest. As the gas or liquid velocity increases in the pipe, a thin film of liquid near the wall creeps up the pipe wall and the interface will have a more tendency to form a curved shape. This fact is shown schematically in Figure 4. The primary reason is that the interface liquid layer

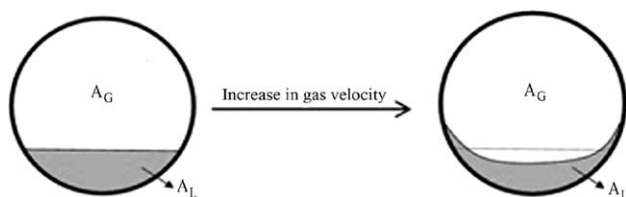


**Figure 4. Effect of gas velocity on forming curvature in interface of gas–liquid.**

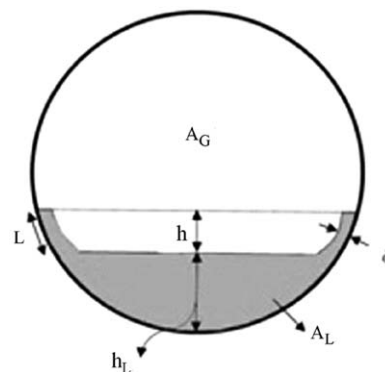


**Figure 5. The gas–liquid pattern considered in this model.**

has a tendency to move with the velocity of interface,  $u_i$ . However, for the points near to the pipe wall, the velocity approaches zero according to no slip condition. Thus, for the points on the interface, which are close to the wall, the velocity head is transformed into static pressure and it makes the liquid creeps up against the pipe wall and forms a thin layer. Figure 5 shows the static head of  $h$  and the thin liquid layer formed near the wall.

As shown in this figure, the interface is predominantly flat except for a thin film near the wall. The thickness of the thin liquid layer which creeps against the wall is assumed to be constant. The flat interface for the regions far from the wall is observed in the experimental study performed by Soleimani and Talaei.<sup>22</sup> Figure 6 gives a few images of this work which have been captured using wire mesh electrical system for different gas and liquid velocities in horizontal pipe. The white and dark points demonstrate liquid and gas regions, respectively.

### Governing equations

The steady-state gas and liquid-phase momentum balance equations can be written as follows:

$$-A_G \left( \frac{dp}{dx} \right)_G - \tau_{wG} S_G - \tau_i S_i - A_G \rho_G g \sin \beta = 0 \quad (1)$$

$$-A_L \left( \frac{dp}{dx} \right)_L - \tau_{wL} S_L + \tau_i S_i - A_L \rho_L g \sin \beta = 0 \quad (2)$$

where  $\rho$  and  $A$  are phase density and cross-sectional area, respectively. The subscript  $G$  and  $L$  stand for gas and liquid phases.  $\beta$  and  $g$  are inclination angle of pipeline and acceleration due to gravity.  $\beta$  is positive for upward and negative for downward pipes.  $p$  is the pressure at each point along the pipeline, respectively.  $S_i$ ,  $S_G$ ,  $S_L$  are the interfacial surface per unit of length for gas–liquid, gas–wall and liquid–wall, respectively.  $\tau_i$ ,  $\tau_G$ , and  $\tau_L$  are the shear stresses between gas–liquid, gas–wall, and liquid–wall, respectively. The average pressure gradients in gas and liquid can be assumed equal:

$$\left( \frac{dp}{dx} \right)_G = \left( \frac{dp}{dx} \right)_L = \left( \frac{dp}{dx} \right) \quad (3)$$

This assumption is generally valid in the absence of interfacial liquid level gradients. Equations 1 through 3 are combined to yield the following form:

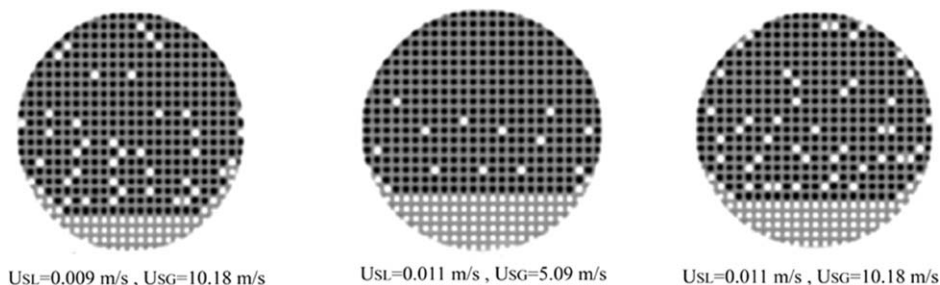


**Figure 6. The images of cross section of water–air flow through a horizontal pipe in different gas and liquid velocities captured by Soleimani and Talaei.<sup>22</sup>**

$$\tau_{wG} \frac{S_G}{A_G} - \tau_{wL} \frac{S_L}{A_L} + \tau_i S_i \left( \frac{1}{A_L} + \frac{1}{A_G} \right) - (\rho_L - \rho_G) g \sin \beta = 0 \quad (4)$$

Equation 4 comprises shear stresses and geometrical parameters ( $A_L$ ,  $A_G$ ,  $S_L$ ,  $S_G$ , and  $S_i$ ). Shear stress terms are defined as follows:

$$\tau_{wL} = \frac{f_{wL} \rho_L u_{SL}^2}{2\alpha^2} \quad (5)$$

$$\tau_{wG} = \frac{f_{wG} \rho_G u_{SG}^2}{2(1-\alpha)^2} \quad (6)$$

$$\tau_i = \frac{f_i \rho_G |u_i - u_L| (u_i - u_L)}{2} = \frac{f_i \rho_G \left| \frac{u_{SG}}{1-\alpha} - \frac{u_{SL}}{\alpha} \right| \left( \frac{u_{SG}}{1-\alpha} - \frac{u_{SL}}{\alpha} \right)}{2} \quad (7)$$

In Eq. 7, it was assumed that there was no slip between gas and liquid interphases and the interface velocity ( $u_i$ ) was very close to the gas velocity ( $u_G$ ). It is well-worth explaining that the slip term, which usually appears in two-phase flow literature, refers to the difference between average gas and liquid velocities. However, the no-slip assumption between gas and liquid interphases in more general sense is almost always applicable except for the case of utilizing surfactant in liquid phase. In this work, it was made the assumption of uniform gas velocity distribution because of strong turbulent mixing effect. It was also assumed that no-slip assumption is valid between gas and liquid interphase. However, it does not mean that there is no difference between average gas and liquid velocities as there is still velocity distribution throughout the liquid phase. In these equations,  $u_{SL}$  and  $u_{SG}$  are superficial liquid and gas velocities, respectively. Geometrical parameters in Eq. 4 are

defined as below based on the gas–liquid pattern shown in Figure 5:

$$A_L = 0.25d^2 \left[ \pi - \cos^{-1} \left( 2 \frac{h_L}{d} - 1 \right) + \left( 2 \frac{h_L}{d} - 1 \right) \sqrt{1 - \left( 2 \frac{h_L}{d} - 1 \right)^2} \right] + 2l\delta \quad (8)$$

$$A_G = \pi \frac{d^2}{4} - \left\{ 0.25d^2 \left[ \pi - \cos^{-1} \left( 2 \frac{h_L}{d} - 1 \right) + \left( 2 \frac{h_L}{d} - 1 \right) \sqrt{1 - \left( 2 \frac{h_L}{d} - 1 \right)^2} \right] + 2l\delta \right\} \quad (9)$$

$$S_L = d \left[ \pi - \cos^{-1} \left( 2 \frac{h_L}{d} - 1 \right) \right] + 2l \quad (10)$$

$$S_G = \pi d - \left\{ d \left[ \pi - \cos^{-1} \left( 2 \frac{h_L}{d} - 1 \right) \right] + 2l \right\} \quad (11)$$

$$S_i = d \sqrt{1 - \left( 2 \frac{h_L}{d} - 1 \right)^2} + 2l \quad (12)$$

In the above equations  $h_L$ ,  $l$ , and  $\delta$  are geometric parameters as shown in Figure 5 and  $\alpha$  is liquid volume fraction. Substituting Eqs. 5 through 12 into Eq. 4 results in an equation with four unknowns of  $\alpha$ ,  $h_L$ ,  $l$ , and  $\delta$ . Therefore, to solve the Eq. 4 for liquid holdup, one needs three more equations to correlate  $\alpha$ ,  $h_L$ ,  $l$ , and  $\delta$  with each other.  $l$  can be found from the following geometric equation:

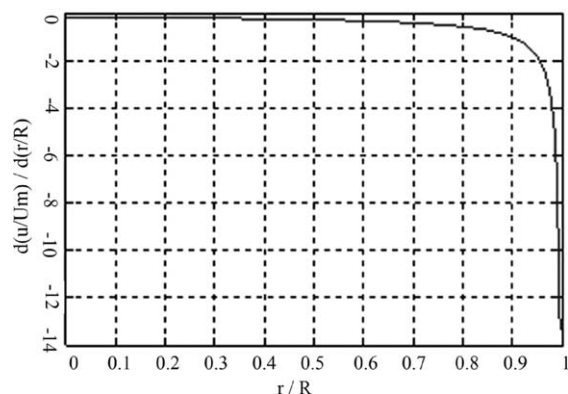


**Figure 7. The variation of liquid velocity versus distance from center of pipe based on one-seventh power Law.**

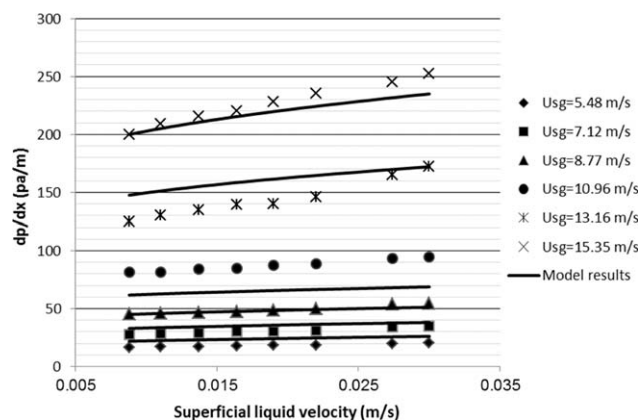


**Figure 8. Air–water experimental data compared with the predictions of presented model in constant superficial gas velocities.**



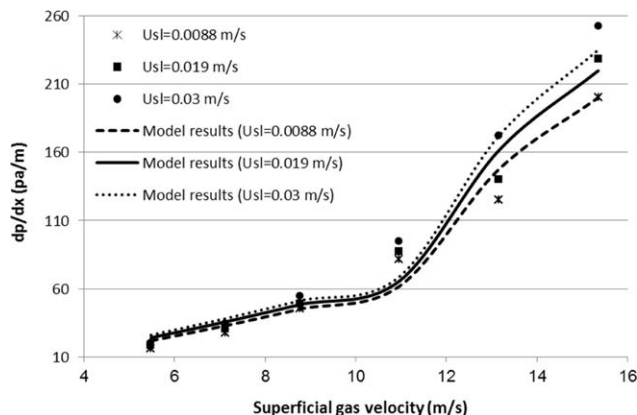


**Figure 9. New model's behavior in prediction of acquired laboratory data where superficial liquid velocity is considered constant.**

$$l = R \left[ \sin^{-1} \left( \frac{h_L + h - R}{R} \right) - \sin^{-1} \left( \frac{h_L - R}{R} \right) \right] \quad (13)$$

In the above equation,  $h$  is the last geometrical parameter as shown in Figure 5.

Once gas and liquid comes into contact in a horizontal pipe at very low gas and liquid velocities, they form a flat interface. As either gas or liquid velocities increases, gas-liquid interface tends to be curved. It can be attributed to the generation of velocity distribution throughout the liquid phase. The layers near the pipe wall flow at lower velocities as a result of wall effect. Consequently, velocity head is transformed into pressure head. This pressure head is provided by raising the liquid to the level which is equal to its respective velocity head. In other words, for the points on the interface, which are close to the wall, the velocity head is transformed into static pressure and it makes the liquid creeps up against the pipe wall and forms a thin layer. The following equation expresses the transformation of this velocity head into liquid static head:

$$\rho_G \frac{u_{SG}^2}{2(1-\alpha)^2} = (\rho_L - \rho_G)gh \quad (14)$$

Left hand of this equation is interface velocity head and right hand is static pressure head. This equation was used to find  $h$ :

$$h = \rho_G \frac{u_{SG}^2}{2(1-\alpha)^2(\rho_L - \rho_G)g} \quad (15)$$

Liquid holdup,  $\alpha$ , in gas-liquid flow through a pipe is defined as the ratio of pipe cross sectional area occupied by liquid to the total cross sectional area. Consequently, the following equation can be written based on geometrical relations for liquid holdup:

$$\alpha = \frac{A_L}{A} = \frac{0.25d^2 \left[ \pi - \cos^{-1} \left( 2 \frac{h_L}{d} - 1 \right) + \left( 2 \frac{h_L}{d} - 1 \right) \sqrt{1 - \left( 2 \frac{h_L}{d} - 1 \right)^2} \right] + 2l\delta}{\pi \frac{d^2}{4}} \quad (16)$$

where  $\delta$  is the thickness of the liquid film formed at the vicinity of the pipe wall. The velocity of liquid at gas-liquid interface can be estimated equal to gas velocity. However, at a very close vicinity of the pipe wall, liquid velocity is declined sharply. As already mentioned, this steep reduction of velocity causes a narrow layer adjacent to the pipe wall to protrude from the main flat interface. Thus, to find the thickness of  $\delta$ , one should determine the point in liquid where the velocity is declined rapidly. The interval between this point and the pipe wall will be equal to  $\delta$ . For this purpose, estimation of velocity distribution in liquid phase could be useful. In this article, the interface velocity has been considered equal to gas velocity. It means that the layer of liquid in contact with gas has the velocity of gas which is high. This high velocity could cause turbulence in liquid phase. Therefore, the flow regime in liquid phase is considered as turbulent flow. In the mechanistic models, although it is tried to cover all important physical rules governing the gas-liquid phenomenon, it is needed to simplify the problem with some valid assumptions. The dimensionless velocity distribution in turbulent flow can be estimated by one-seventh power law as below:

$$\frac{u}{u_{\max}} = \left( 1 - \frac{r}{R} \right)^{1/7} \quad (17)$$

Figure 7 shows the plot of  $\frac{d(\frac{u}{u_{\max}})}{d(\frac{r}{R})}$  versus  $\frac{r}{R}$  which was drawn based on the above equation. As can be seen in this figure, the variation of  $\frac{d(\frac{u}{u_{\max}})}{d(\frac{r}{R})}$  at  $t = \frac{r}{R} = 0.95$  becomes very steep. Therefore, the thickness of  $\delta$  can be estimated equal to:

$$\delta = 0.05 \frac{d_L}{2}, \quad d_L = \frac{4A_L}{S_L} \quad (18)$$

The gas-liquid interface is curved mainly because of velocity distribution in liquid phase. The only thorough way to incorporate this effect into the model is direct numerical simulation which makes the model very complicated. Although mechanistic models are developed based on the physical principles underling gas-liquid flow phenomena, they should be still so simple that can be used in lengthy two-phase flow calculations. In other words, there should be a tradeoff between simplicity and accuracy of a mechanistic model. As a result, the model needs a simple way for prediction of break point in liquid velocity distribution. One simple method is to use one-seventh power law using hydraulic

**Table 1. The Experimental Data Sets Used for Comparison**

Researcher	Kind of Data	Pipe Diameter(m)	Gas/Liquid Flows	Number of Data
Badie et al. <sup>3</sup>	Pressure drop Liquid hold up	0.078	Air-water Air-oil	124
Meng <sup>24</sup>	Pressure drop	0.051	Air-oil	11
Soleimani and Talaei <sup>22</sup>	Liquid hold up	0.0254	Air-water	16
Fan <sup>20</sup>	Pressure drop Liquid hold up	0.051 0.150	Air-water	302
	Wetted wall fraction			
Chen et al. <sup>14</sup>	Wetted wall fraction	0.0779	Air-kerosene	48

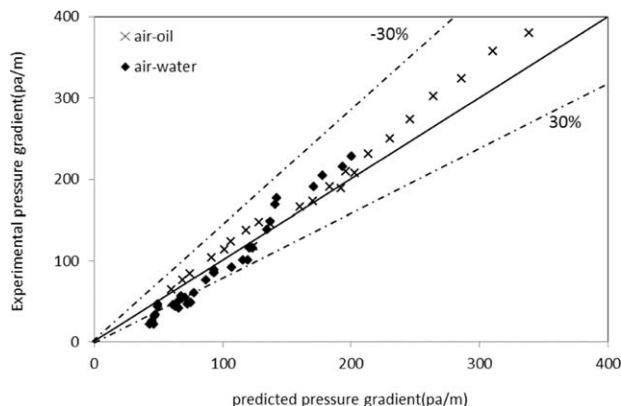


**Figure 10.** The comparison of the results of the present model with pressure drop experimental data measured by Badie el al.<sup>3</sup>

diameter of liquid phase. Based on this fact, some previous researchers have estimated velocity profile in gas–liquid flow systems using correlations for single flow in pipe. Fan<sup>20</sup> assumed a logarithmic velocity profile for turbulent flow in liquid phase for a gas–liquid flow with low liquid loading system. For further evaluation, a logarithmic velocity profile was also tried for estimation of velocity profile in liquid phase to find the break point in liquid velocity distribution. Interestingly, it was revealed that using both correlations culminated in approximately the same results and there was no significant difference between model's predictions (see Appendix A).

In the end, Eqs. 4 through 18 were solved simultaneously for the unknown parameters of  $h_L$ ,  $l$ ,  $\delta$ ,  $\alpha$ , and  $h$ . To find pressure gradient either Eq. 1 or 2 can be applied.

### Friction factors

The way of predicting liquid–wall, gas–wall and gas–liquid friction factors appeared in Eqs. 5 through 7 is of great importance in any two-phase flow model. Many correlations for prediction of liquid–wall, gas–wall, and gas–liquid friction factors can be found in the literature. To find the best correlations for the present model, 30 correlations were examined by comparing the results of the model with some experimental data for pressure drop and liquid holdup. Through this comparison it was revealed that using different correlations for prediction of liquid–wall friction factor did

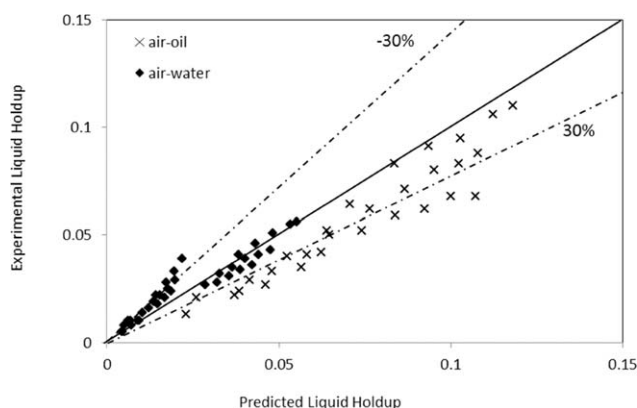


**Figure 11.** The comparison of the results of the present model with liquid holdup experimental data measured by Badie el al.<sup>3</sup>

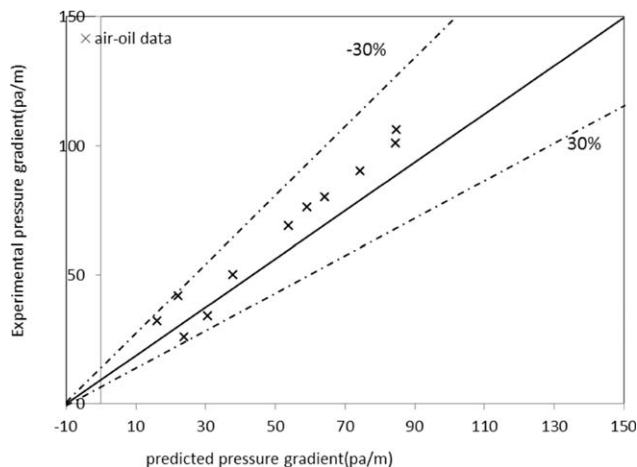


**Figure 12.** The comparison of the results of the present model with pressure drop experimental data measured by Meng.<sup>24</sup>

not have considerable effect on the result of the model. In other word, using correlations which predict gas–wall and gas–liquid friction factors accurately have a stronger impact on the model results. It is attributed to the low loading of liquid for this case. It was also found that the correlation used by Taitel and Dukler<sup>7</sup> for prediction of liquid–wall friction factor was provided the lowest average relative error. This correlation, which was recognized to be appropriate for the present model, is as follows:

$$f_L = C_L \text{Re}_L^{-n} \quad (19)$$

Where  $C_L = 0.046$  and  $n = 0.2$  for the turbulent flow and  $C_L = 16$  and  $n = 1.0$  for the laminar flow.

For two-phase flow with low liquid loading most of the cross sectional area of the pipe is occupied by gas. As a result, it is supposed that the friction factor correlation which provides better results for gas single-phase flow can be more suitable for such models too. Thus, a set of pressure drop experimental data was obtained for gas single-phase flow by Banafi and Talaei.<sup>23</sup> Different gas friction factor correlations were examined by comparing the computational results with this set of experimental data. This comparison revealed that

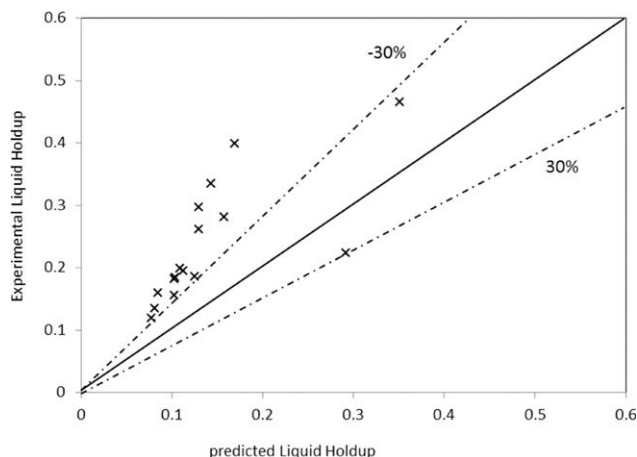


**Figure 13.** The comparison of the results of the present model with liquid holdup experimental data measured by Soleimani and Talaei.<sup>22</sup>

**Table 2. The Comparison of the Presented Model's Predictions Using New Correlation for  $f_i$  with the Ones Using the Correlation Proposed by Taitel and Dukler<sup>7</sup>**

Researcher	Kind of Data	Gas/Liquid Flows	Average Relative Error (%)	
			$f_i$ (Taitel–Dukler)	$f_i$ (new)
Badie et al. <sup>3</sup>	Pressure drop	Air/water	30.72	28.1
Badie et al. <sup>3</sup>	Pressure drop	Air/oil	53.84	8.49
Meng <sup>25</sup>	Pressure drop	Air/oil	47.63	22.86
Badie et al. <sup>3</sup>	Liquid holdup	Air/water	41.13	18.55
Badie et al. <sup>3</sup>	Liquid holdup	Air/oil	146.37	34.70
Soleimani and Talaei <sup>22</sup>	Liquid holdup	Air/water	56.69	42.40

the following correlation proposed by Taitel and Dukler<sup>7</sup> for gas–wall friction factor provided the best results:

$$f_G = C_G Re_G^{-m} \quad (20)$$

Where  $C_G=0.046$  and  $m=0.2$  for the turbulent flow and  $C_G=16$  and  $m=1.0$  for the laminar flow.

To improve the capability of the present model, new correlation for  $f_i$  was proposed. Solving Eqs. 4–18 simultaneously and also using Eqs. 19 and 20 for liquid–wall and gas–wall friction factors, respectively, all parameters in Eq. 4 will be known except  $\frac{dp}{dx}$  and  $f_i$ . Through this equation,  $f_i$  was correlated by fitting to obtained experimental data of pressure drop. The following equation was obtained through this fitting:

$$f_i = \frac{0.02066}{\left(\log\left(\frac{15}{Re_G} + \frac{k}{3.71d}\right)\right)^2}, \quad \frac{k}{d} = 0.01249 \frac{\alpha}{\theta} \quad \text{when } Re_{GS} \geq 17758$$

$$f_i = \frac{0.07452}{\left(\log\left(\frac{15}{Re_G} + \frac{k}{3.71d}\right)\right)^2}, \quad \frac{k}{d} = 3.5196 \frac{\alpha}{\theta} \quad \text{when } Re_{GS} < 17758 \quad (21)$$

Where  $k$  is the apparent roughness due to ripples formed on the surface of the liquid film. In the above equation,  $k$

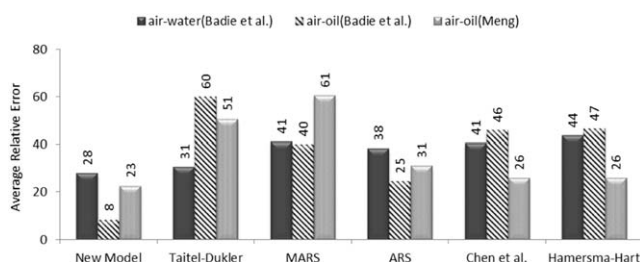
will be larger if the gas velocity and hence gas Reynolds number increase. Increasing gas velocity causes larger waves on the liquid film surface and higher apparent roughness.

The most interesting feature of the new model is that it comes close to Olieman's theory, a thin film covering a part of wall, at very low liquid loading and high gas velocity, and it approaches Taitel–Dukler flat interface at higher liquid loading and lower gas velocities. Consequently, the model will be expected to be valid for a wider range of gas and liquid velocities.

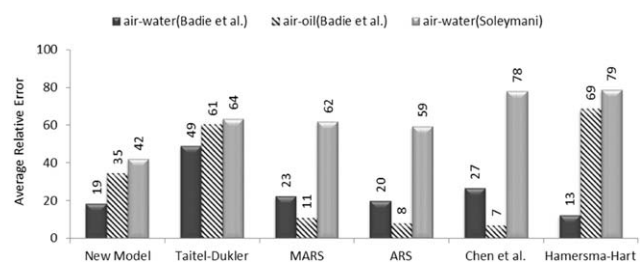
## Result and Discussion

Figure 8 illustrates air–water experimental data compared with the predictions of presented model in constant superficial gas velocities. Figure 9, also, indicates the new model's behavior in prediction of several sets of acquired laboratory data where superficial liquid velocity considers constant. These experimental data follows the trend established in the previous works that pressure gradients increase with rising gas and liquid velocities.

In this section, the performance of the new model along with several well-known models existed in the literature which are all applicable in stratified flow regime were compared with experimental data in terms of pressure drop and liquid holdup. The used experimental data were presented in Table 1. All of these data gathered for evaluation of capability of different models are placed in stratified flow regime in a flow pattern map.



**Figure 14. The comparison between the performance of several well-known models and three sets of experimental data for pressure drop.**



**Figure 15. The comparison between the performance of several well-known models and three sets of experimental data for liquid holdup.**

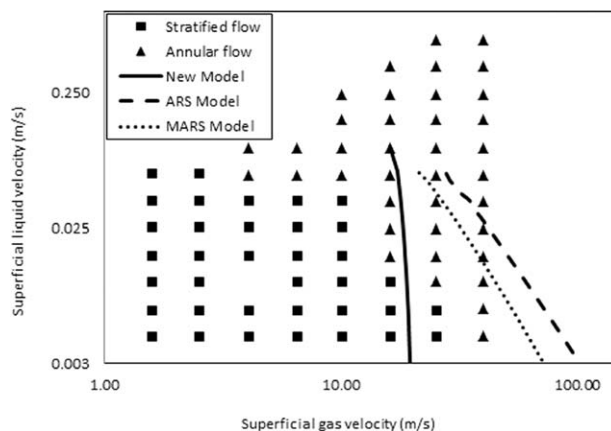


**Figure 16. The comparison of the predicted stratified-annular border line with the experimental data obtained by Barnea et al.<sup>25</sup> for 1-in. pipe.**

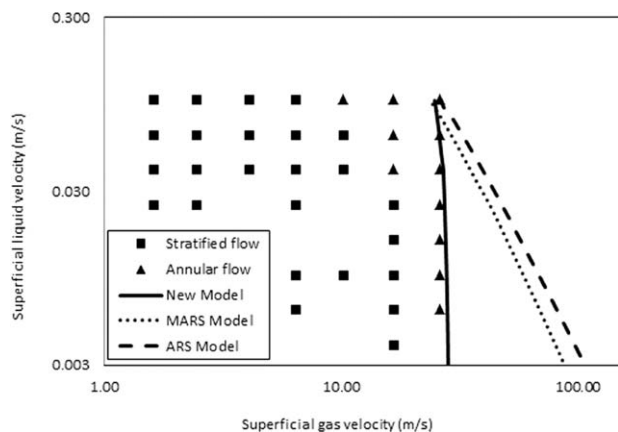


**Figure 17.** The comparison of the predicted stratified-annular border line with the experimental data obtained by Barnea et al.<sup>25</sup> for 2-in. pipe.

These data includes pressure drop and liquid holdup information on gas-liquid flow through pipes having different diameters with low liquid loading. To make a thorough comparison, the effort was made to collect the experimental data covering a vast range of operating conditions. Figures 10–13 compare the result of the presented model with the experimental data. These figures demonstrate that the new model is capable of making a reasonable prediction of pressure drop.

To show how much the new correlation for  $f_i$  improves the results of new model, the presented model's predictions obtained using new correlation were compared with the ones attained using Taitel-Dukler correlation,<sup>7</sup> which provided lowest error among other correlations introduced in the literature when used in new model. The relative errors of new model's results in these two states are shown in Table 2.

As Table 2 shows, in spite of tuning the new correlation for  $f_i$  for accurately predicting air-water pressure loss experimental data in 1 in. pipe diameter, it demonstrates higher ability in comparison with Taitel-Dukler<sup>7</sup> correlation presented for  $f_i$  in prediction of both pressure drop and liquid holdup data for larger pipes and the systems other than air-water.

Figures 14 and 15 draw comparison among several models with three different sets of experimental data. As can be seen from these figures, the new model provides better prediction for pressure drop than the others do. It is also more successful in predicting the liquid holdup experimental data of Soleimani and Talaei.<sup>22</sup>

The average relative errors of all models in predicting these data are higher than 40%. It can be attributed to the fact that the experimental data includes the liquid holdups as

high as 0.4. However, these models were adapted for gas-liquid flow with low liquid loading. One of the prominent features of the presented model is its capability of providing better prediction for a wide range of liquid holdup. The outcome of these comparisons reveals that although the model was fitted to the experimental data of pressure drop for air-water system in 1 in. pipe, it provides quite reasonable results for the conditions beyond that, that is, two-phase system other than air-water and pipe size larger than 1 in. It can be ascribed to the mechanistic method used to predict liquid-gas interface shape in the present model. Indeed, the liquid-gas interface shape predicted by the present model approaches thin film layer at low liquid holdups while it becomes close to flat surface for higher liquid holdup. Thus, the new model offers much more realistic picture of gas-liquid interface than the previous models do. To support this claim, the ability of the new model was examined for predicting the border of turning stratified into annular flow pattern. Figures 16 and 17 show the border line predicted by ARS,<sup>2</sup> MARS<sup>15</sup> and the presented model, and their comparison with the experimental data of Barnea et al.<sup>25</sup> These lines calculated based on different models' prediction of wetted wall fraction. When the predicted wetted wall fraction approaches unity, flow regime turns from stratified into annular flow. Evidently, the new model provides more reasonable prediction than two other models do. The more accurate prediction by solid line than dashed lines is obvious especially in low liquid velocities. Better predictions provided by new model can lend support to the fact that the new model can perform better than the previous models even in the vicinity of turning point to annular flow pattern.

For further evaluation, the results of the new model in addition to MARS, ARS and Taitel-Dukler were compared with the experimental pressure drop data of Meng<sup>24</sup> for the region close to annular flow pattern. This comparison indicates that the new model is more powerful than the rest of the models as shown in Table 3.

Fan<sup>20</sup> performed a set of experiments to measure pressure loss and liquid hold up for air-water flow in 2- and 6-in. pipe diameters. Figures 18 and 19 compare the results of the presented model with these data. As can be seen from these figures, new model has reasonable predictions for both pressure drop and liquid hold up in 6-in. pipe diameter which demonstrates the scalability of the model. It should be mentioned that the average relative errors in prediction of pressure loss and liquid hold up data in 6-in. pipe diameter are 18.8 and 22.4% respectively.

The correct prediction of wetted perimeter can be considered as a good measure of the capability of a model for accurately predicting gas-liquid interface shape. Figures 20 and 21 show the comparison of wetted perimeter predicted using the new model with the experimental data of Chen and

**Table 3.** The Comparison of the Results of the Model with the Experimental Data of Meng<sup>24</sup> Which was Obtained for the Regions Near to Annular Flow

U <sub>ls</sub> (m/s)	U <sub>gs</sub> (m/s)	Flow Pattern	dp/dx (pa/m)	Relative Error (%)			
				New Model	MARS	ARS	Taitel-Dukler
15.1	0.0014	SW-AN	144	25.86	40.87	37.54	50.72
15.2	0.0023	SW-AN	153	25.34	39.10	36.04	52.56
15.2	0.0049	SW-AN	163	22.96	32.11	30.73	54.39
15.2	0.0111	SW-AN	176	19.38	15.11	21.09	56.05



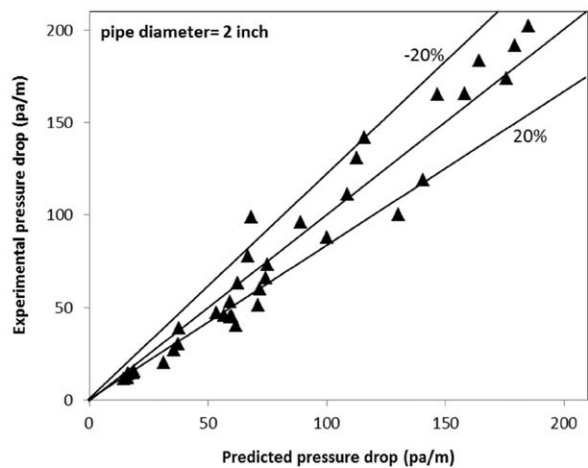
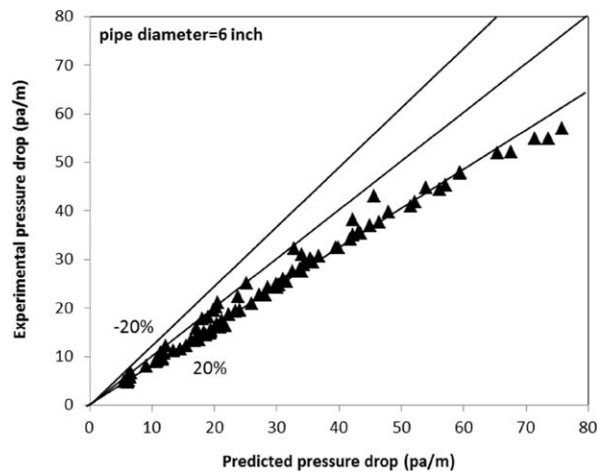


Figure 18. The comparison of the results of the present model with pressure drop experimental data measured by Fan.<sup>20</sup>

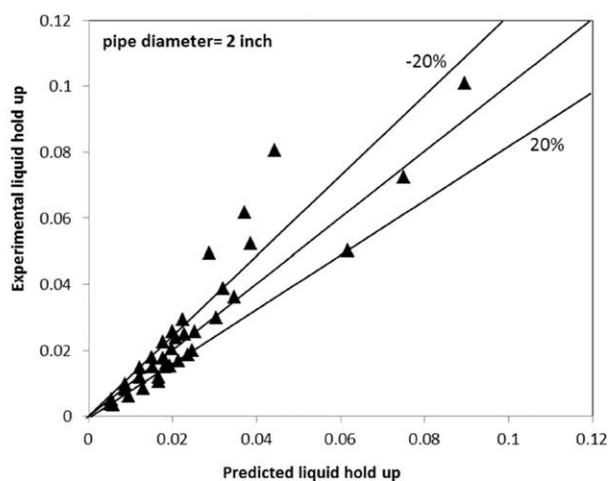
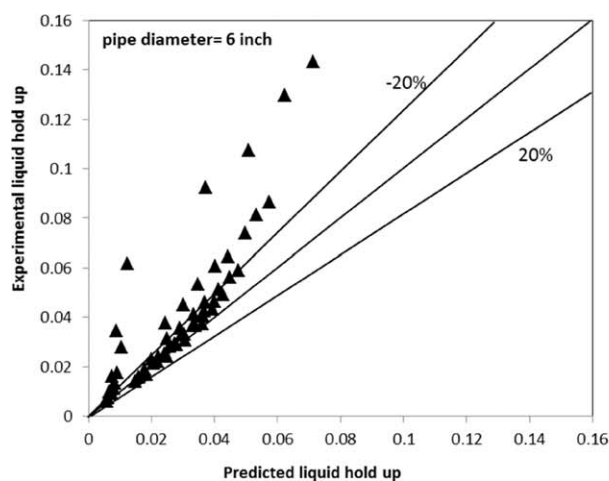


Figure 19. The comparison of the results of the present model with liquid hold up experimental data measured by Fan.<sup>20</sup>

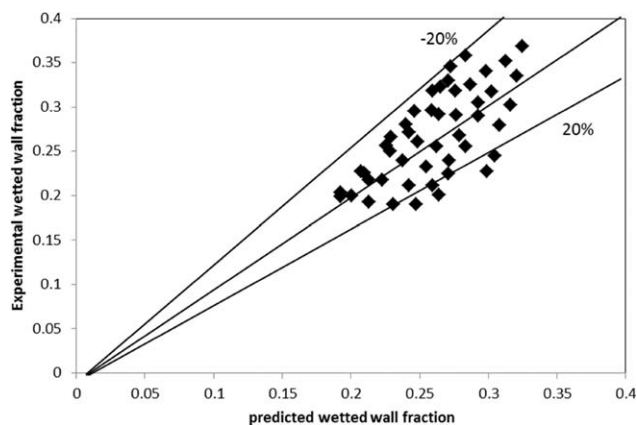


Figure 20. The comparison of the wetted wall perimeter obtained by the model with the experimental data obtained by Chen et al.<sup>14</sup> for air-kerosene system in 0.0779-m pipe.

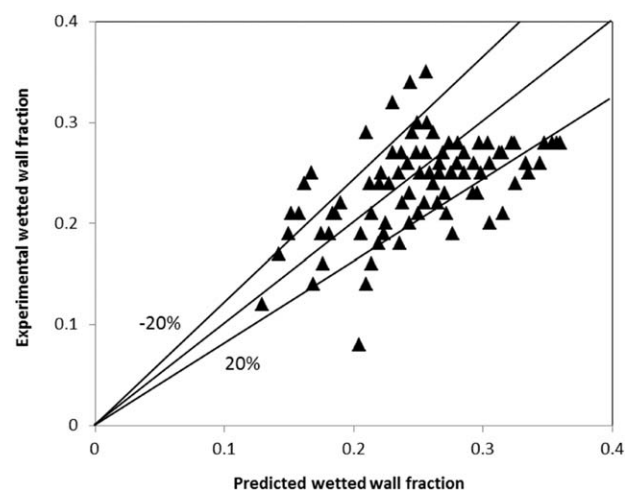


Figure 21. The comparison of the wetted wall perimeter obtained by the model with the experimental data obtained by Fan<sup>20</sup> for air-water system in 6-in. pipe.

et al.<sup>14</sup> for air–kerosene flow through a pipe with the diameter of 0.0779 m and Fan<sup>20</sup> for air–water flow in a 6 in. pipe diameter. The average relative error in predicting these experimental data were 11.92 and 19.4% respectively which are reasonably appropriate.

## Conclusion

A new model was introduced to predict pressure drop and liquid holdup in gas–liquid flow through a pipeline with low liquid loading. This model was primarily developed based on the physical fact that the gas velocity is the key factor in shaping gas–liquid interface. The new model is capable of providing satisfactory results for both pressure drop and liquid holdup for a wide range of operating conditions, that is, different pipe sizes and gas–liquid systems. The primary feature of the presented model is its applicability in a vast range of liquid holdups. In addition, the introduced model can make better prediction of the stratified-annular transformation. This fact supports the claim that the new model has better performance in the border region which is close to annular flow pattern than the previous models do. The model also provides acceptable prediction of wetted wall perimeter of the pipe.

## Literature Cited

1. Zhang HQ, Sarica C. Low liquid loading gas/liquid pipe flow. *J Nat Gas Sci Eng*. 2011;3:413–422.
2. Hart NP, Hamersma PJ, Fortuin JMH. Correlations predicting frictional pressure drop and liquid holdup during horizontal gas-liquid pipe flow with small liquid holdup. *Int J Multiphase Flow*. 1989;15:947–964.
3. Badie S, Hale CP, Lawrence CJ, Hewitt GF. Pressure gradient and holdup in horizontal two-phase gas-liquid flows with low liquid loading. *Int J Multiphase Flow*. 2000;26(9):1525–1543.
4. Lockhart RW, Martinelli RC. Proposed correlation of data for isothermal two-phase, two-component flow in pipes. *Chem Eng Prog*. 1949;45:39–48.
5. Hughmark GA. Holdup in gas/liquid flow in horizontal pipes. *Chem Eng Prog*. 1962;58:62–75.
6. Beggs HD, Brill JP. A study of two-phase flow in inclined pipelines. *J Pet Technol*. 1973;25:607–617.
7. Taitel Y, Dukler AE. A model for predicting flow transition regime transitions in horizontal and near horizontal gas liquid flow. *AIChE J*. 1976;22:47–54.
8. Oliemans RVA. *Two-Phase Flow in Gas Transmission Pipeline*. Mexico City, ASME Paper, 1976:19–24.
9. Cheremisinoff NP, Davis EJ. Stratified turbulent-turbulent gas-liquid flow. *AIChE J*. 1975;21(1):48–56.
10. Shoham O, Taitel Y. Stratified turbulent-turbulent gas-liquid flow in horizontal and inclined pipes. *AIChE J*. 1984;30:377–385.

11. Hamersma PJ, Hart J. A pressure drop correlation for gas/liquid pipe flow with small liquid holdup. *Chem Eng Sci*. 1986;42:1187–1196.
12. Issa RI. Prediction of turbulent, stratified, two-phase flow in inclined pipes and channels. *Int J Multiphase Flow*. 1988;14:141–154.
13. Baker A, Nielsen K, Gabb A. Field data test new holdup, pressure-loss calculations for gas-condensate pipelines. *Oil Gas J*. 1988;86:12.
14. Chen XT, Cai XD, Brill JP. Gas-liquid stratified-Wavy flow in horizontal pipeline. *J Energy Resour Technol*. 1997;119:209–216.
15. Grolman E, Fortuin JMH. Gas-liquid flow in slightly inclined pipes. *Chem Eng Sci*. 1997;52:4461–4471.
16. Vlachos NA, Paras SA, Karabelas AJ. Prediction of holdup, axial pressure gradient and wall shear stress in wavy stratified and stratified/atomization gas/liquid flow. *Int J Multiphase Flow*. 1999;25:365–376.
17. Asante B. Two phase flow: accounting for the presence of liquids in gas pipeline simulation. In: PSIG Annual Meeting, Portland, Oregon, 23–25 October, 2002; Document ID PSIG-02W3.
18. Meng W, Chen X, Kouba G, Cem S, Brill G. Experimental study of low liquid loading gas-liquid flow in near horizontal pipes. *SPE Prod Facil*. 2001;16(4):240–249.
19. Talaie MR, Soleimani Deilamani K. A new approach for modeling of gas-condensate flow through pipelines under industrial operating conditions. *J Nat. Gas Sci*. 2014;21:540–555.
20. Fan Y. An investigation of low liquid loading gas-liquid stratified flow in near-horizontal pipes: University of Tulsa, Tulsa, PhD Dissertation, 2005.
21. Banafi A, Talaie MR, Ghafoori MJ. A comprehensive comparison of the performance of several popular models to predict pressure drop in stratified gas-liquid flow with low liquid loading. *J Nat. Gas Sci. Eng*. 2014;21:433–441.
22. Soleimani deilamani K, Talaie MR. Experimental study and modeling of liquid curvature in gas-condensate (two-phase) flow with low liquid loading for stratified and annular regimes. University of Isfahan, Isfahan, Iran. M.Sc. Thesis, 2011.
23. Banafi A, Talaie MR. Experimental and theoretical investigation of pressure drop and liquid holdup in gas-liquid flow through pipes with low liquid loading. University of Isfahan, Isfahan, Iran. M.Sc. Thesis, 2012.
24. Meng W. Low-liquid loading gas-liquid two-phase flow in near horizontal pipes. University of Tulsa, Tulsa, PhD Dissertation. 1999.
25. Barnea D, Shoham O, Taitel Y. Flow pattern transition for gas-liquid flow in horizontal and inclined pipes. *Int J Multiphase Flow*. 1980;6:225–217.

## APPENDIX

In the present model, the break point of liquid velocity distribution (and not the whole velocity distribution) has been predicted using one-seventh power law using hydraulic diameter of liquid phase. As mentioned before, for further evaluation, a logarithmic velocity profile was also tried for estimation of velocity profile in liquid phase to find the break

**Table A1. The Comparison of the Average Relative Error of the Model Predictions Using One-Seventh Power Law with the Ones Using Logarithmic Velocity Profile**

Researcher	Kind of Data	Pipe Diameter	Gas/Liquid Flows	Average Relative Error (%)	
				1/7 Power Law	Logarithmic
Badie et al. <sup>3</sup>	Pressure drop	0.078	Air–water	28.10	28.16
Badie et al. <sup>3</sup>	Pressure drop	0.078	Air–oil	8.49	8.43
Meng <sup>24</sup>	Pressure drop	0.051	Air–oil	22.86	22.82
Fan <sup>20</sup>	Pressure drop	0.1496	Air–water	18.84	18.97
Fan <sup>20</sup>	Pressure drop	0.051	Air–water	19.05	19.07
Badie et al. <sup>3</sup>	Liquid holdup	0.078	Air–water	18.55	18.49
Badie et al. <sup>3</sup>	Liquid holdup	0.078	Air–oil	34.70	34.67
Soleimani and Talaie <sup>22</sup>	Liquid holdup	0.0254	Air–water	42.40	42.31
Fan <sup>20</sup>	Liquid holdup	0.1496	Air–water	22.42	22.31
Fan <sup>20</sup>	Liquid holdup	0.051	Air–water	22.46	22.48

point in liquid velocity distribution. In this section, the results of new model in predicting different experimental data in these two states are shown in Table A1. As can be seen from this table, using both correlations (one-seventh power law and logarithmic velocity profile) culminated in approximately the

same results and there was no significant difference between model's predictions.

*Manuscript received Feb. 3, 2014, and revision received Oct. 19, 2014.*

---